• Original Paper •

New Record Ocean Temperatures and Related Climate Indicators in 2023

Lijing CHENG[*1], John ABRAHAM[2], Kevin E. TRENBERTH[3,4], Tim BOYER[5], Michael E. MANN[6],
Jiang ZHU[1,2], Fan WANG[7], Fujiang YU[8], Ricardo LOCARNINI[5], John FASULLO[3], Fei ZHENG[1],
Yuanlong LI[7], Bin ZHANG[7,9], Liying WAN[8], Xingrong CHEN[8], Dakui WANG[8], Licheng FENG[8],
Xiangzhou SONG[10], Yulong LIU[11], Franco RESEGHETTI[12], Simona SIMONCELLI[13],
Viktor GOURETSKI[1], Gengxin CHEN[14], Alexey MISHONOV[5,15], Jim REAGAN[5],
Karina VON SCHUCKMANN[16], Yuying PAN[1], Zhetao TAN[1], Yujing ZHU[1],
Wangxu WEI[1], Guancheng LI[17], Qiuping REN[7], Lijuan CAO[18], and Yayang LU[19]

[1]*International Center for Climate and Environment Sciences, Institute of Atmospheric Physics,
Chinese Academy of Sciences, Beijing 100029, China*
[2]*University of St. Thomas, School of Engineering, Minnesota 55105, USA*
[3]*NSF National Center for Atmospheric Research, Boulder, Colorado 80307, USA*
[4]*University of Auckland, Auckland 1010, New Zealand*
[5]*National Oceanic and Atmospheric Administration, National Centers for Environmental Information,
Silver Spring, Maryland 20910, USA*
[6]*Department of Earth and Environmental Science, University of Pennsylvania, Philadelphia, Pennsylvania 19104, USA*
[7]*Institute of Oceanology, Chinese Academy of Sciences, Qingdao 266071, China*
[8]*National Marine Environmental Forecasting Center, Ministry of Natural Resources of China, Beijing 100081, China*
[9]*Oceanographic Data Center, Chinese Academy of Sciences, Qingdao 266071, China*
[10]*College of Oceanography, Hohai University, Nanjing 210098, China*
[11]*National Marine Data and Information Service, Tianjin 300171, China*
[12]*Italian National Agency for New Technologies, Energy and Sustainable Economic Development,
S. Teresa Research Center, Lerici 19032, Italy*
[13]*Istituto Nazionale di Geofisica e Vulcanologia, Sede di Bologna, Bologna 40128, Italy*
[14]*South China Sea Institute of Oceanology, Chinese Academy of Sciences, Guangzhou 510301, China*
[15]*ESSIC/CISESS-MD, University of Maryland, College Park, MD, 20740, USA*
[16]*Mercator Ocean International, Toulouse 31400, France*
[17]*Eco-Environmental Monitoring and Research Center, Pearl River Valley and South China Sea Ecology and Environment
Administration, Ministry of Ecology and Environment, PRC, Guangzhou 510611, China*
[18]*National Meteorological Information Center, China Meteorological Administration, Beijing 100081, China*
[19]*International Research Center of Big Data for Sustainable Development Goals, Beijing 100094, China*

ABSTRACT

The global physical and biogeochemical environment has been substantially altered in response to increased atmospheric greenhouse gases from human activities. In 2023, the sea surface temperature (SST) and upper 2000 m ocean heat content (OHC) reached record highs. The 0–2000 m OHC in 2023 exceeded that of 2022 by 15 ± 10 ZJ (1 Zetta Joules = 10^{21} Joules) (updated IAP/CAS data); 9 ± 5 ZJ (NCEI/NOAA data). The Tropical Atlantic Ocean, the Mediterranean Sea, and southern oceans recorded their highest OHC observed since the 1950s. Associated with the onset of a strong El Niño, the global SST reached its record high in 2023 with an annual mean of ~0.23°C higher than 2022 and an astounding > 0.3°C above 2022 values for the second half of 2023. The density stratification and spatial temperature inhomogeneity indexes reached their highest values in 2023.

---

* Corresponding author: Lijing CHENG
  Email: chenglij@mail.iap.ac.cn

Article Highlights:

• In 2023, the global annual mean SST and upper 2000 m ocean heat content were the highest ever recorded by modern instruments.
• Other oceanic indices, including density stratification and spatial temperature inhomogeneity, attained record highs.
• A strong El Niño developed during 2023 and influenced warming and salinity anomaly patterns.

---

1. Introduction

The increase in carbon dioxide (CO_2) and other greenhouse gases in the atmosphere from human activities has led to an increase in longwave radiation trapped within the Earth system, resulting in an increase in the difference between incoming and outgoing radiation at the top of the atmosphere and causing an Earth Energy Imbalance (EEI) (Trenberth et al., 2014; Gulev et al., 2021). With about 90% of the excess heat accumulated in the Earth system deposited in the world's ocean, EEI causes rising ocean temperatures and increasing ocean heat content (OHC) (Rhein et al., 2013; Johnson et al., 2018; Von Schuckmann et al., 2020; Loeb et al., 2021; Cheng et al., 2023). Both OHC and the closely associated sea level rise (SLR) are robust indicators of climate change because they have larger forced signal-to-noise ratios than surface temperature change (Cheng et al., 2018). OHC also plays essential roles in Earth's energy, water, and carbon cycles (Cheng et al., 2022a) and significantly affects human society (Abraham and Cheng, 2022).

Further, ocean freshwater change, reflected in changes in ocean salinity, aggregates changes in the atmospheric water cycle and ocean circulation, and these changes, along with temperature changes, regulate the ocean currents and impact the vertical stability of the ocean. Ocean salinity trends are generally characterized by a "fresh gets fresher, salty gets saltier" change pattern, meaning areas that are currently fresh are becoming fresher, and areas that are currently salty are becoming more saline (Durack and Wijffels, 2010). This process can be quantified by a "salinity-contrast" (SC) index that calculates the salinity difference between the higher and lower salinity regions compared to a global average (Cheng et al., 2020).

These ocean temperature and salinity changes are not spatially homogeneous. As the changes are non-uniform, the variance of the three-dimensional upper 2000 m ocean temperature fields have increased (Ren et al., 2022). Vertically, the ocean temperature and density structures are altered, leading to vertical stratification changes (Li et al., 2020a), which in turn impact the vertical exchanges of energy, water, carbon, nutrients, and other substances.

The year 2023 began as the third year of a prolonged La Niña that faded by April, as sea surface temperatures (SSTs) in the tropical central and eastern Pacific rose with the onset of a new major El Niño (Fig. 1). By late 2023, the El Niño was classed as "strong" (> 1.5°C for Oceanic Niño Index), with predicted Niño3.4 SSTs exceeding 1.8°C in
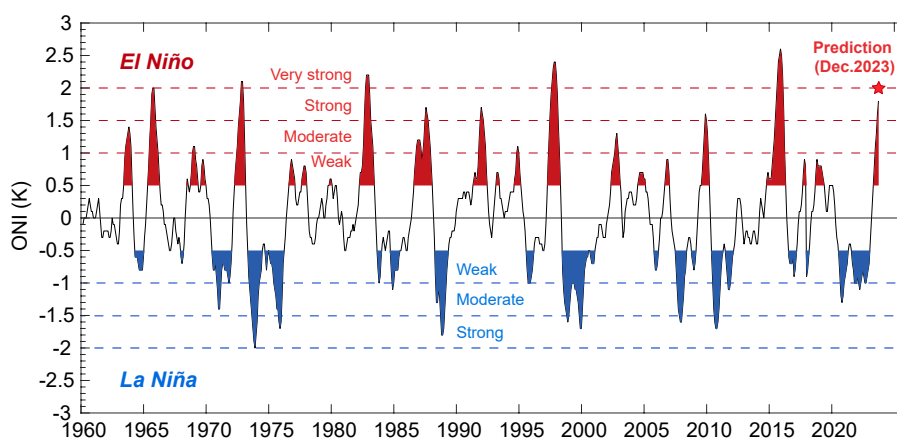
Fig. 1. An ENSO index (Oceanic Niño Index, ONI), calculated based on a 3-month running mean of Extended Reconstructed Sea Surface Temperature, version 5 (ERSST.v5): SST anomalies in the Niño3.4 region (5°N–5°S, 120°–170°W)] (shading) [data updated from Huang et al. (2017)]. The prediction for the December 2023 ONI is based on the IAP ENSO ensemble prediction system (Zheng and Zhu, 2016; Li et al., 2023).

November and December 2023 (Fig. 1). The CO_2 concentration in the atmosphere continued to increase in 2023 and is more than 50% above preindustrial levels. At Mauna Loa, Hawaii, the November 2023 mean rose to 420.46 parts per million by volume (ppm), an increase of about 3 ppm compared to November 2022 (https://gml.noaa.gov/ccgg/trends/). The EEI has remained above 1 W m^{-2} over recent years (Loeb et al., 2022). This equals an energy increase of ~16 ZJ yr^{-1} (1 ZJ = 10^{21} J). If the heating below 2000 m is about 1 ZJ yr^{-1} (Purkey and Johnson, 2010) and 90% of the EEI goes into the ocean, then 13.5 ZJ yr^{-1} is expected in the ocean above 2000 m depth.

Very high SSTs in the extratropics in 2023 were at least in part a consequence of the prior La Niña, as cool surface temperatures reduced tropospheric temperatures and outgoing longwave radiation. In the North Pacific, high ocean temperatures fueled the atmospheric rivers and "rain bombs" that led to extensive flooding but also relief from long-standing drought in many parts of western North America. Severe flooding also occurred in New Zealand, Beijing/China, Alaska, India, Italy, Slovenia, Japan, Vermont, Kenya, and East Africa. Record heatwaves occurred in the southern United States, China, India, southern Europe (Spain, Portugal, Italy, Greece, France) and elsewhere. Wildfires also accompanied several areas that exhibited record heat and/or drought during 2023. Many nations set all-time temperature records and record low sea ice was recorded throughout the southern winter around Antarctica. The Atlantic hurricane season was vigorous, especially considering it was an El Niño year when storm activity would usually be suppressed. In the East Pacific, hurricane Otis developed at a record rate to a category 5 storm in less than one day before making landfall near Acapulco, Mexico, in late October. The results of many of these events have been devastating in terms of lives lost, disruption, and damage. These climatic changes have profound societal and ecological consequences (Abraham et al., 2022).

This paper provides an update on various oceanic changes in 2023 using two different data products: (1) the Institute of Atmospheric Physics (IAP) at the Chinese Academy of Sciences (CAS) (Cheng et al., 2017, 2020; Li et al., 2020a); (2) National Centers for Environmental Information (NCEI) at the National Oceanic and Atmospheric Administration (NOAA) (Levitus et al., 2012). We include the OHC, SST, SC index, stratification, and temperature spatial inhomogeneity indexes to describe ocean changes in 2023.

2. Data and methods

The source data are obtained from in situ measurements made available through the World Ocean Database (WOD) (Boyer et al., 2018), the primary data source for all data products. The main subsurface observing system since 2005 is the profiling floats from the Argo program (Argo, 2023), whereas other data sources, including XBTs from ships of opportunity, conductivity–temperature–depth (CTD) data

from research ships, instrumented animals, gliders, moored buoys, and ice-tethered profilers, augment observations globally and are primary sources in shallow seas/continental shelves, and high-latitude seasonal ice covered areas. The differences between the data products arise from additional in situ observations owned by the data center, data quality control (QC), climatology, vertical interpolation, gap-filling, and other data processing techniques (Abraham et al., 2013; Boyer et al., 2016; Cheng et al., 2022a). All instrumental data are used for the IAP/CAS and NCEI/NOAA products. This paper presents the most up-to-date information from IAP/CAS and NCEI/NOAA for 2023, incorporating the latest data quality processing and mapping techniques. Both the IAP/CAS and NCEI/NAA datasets are monthly gridded products, have 1° × 1° horizontal resolution, and cover the ocean's upper 2000 m.

IAP introduced a major update in 2023 based on a previous version in Cheng et al. (2017); the data quality-control named the CAS-Ocean Data Center (CODC) Quality Control system—CODC-QC (Tan et al., 2023), where only the "good" data (flag = 0) are used. XBT biases have been corrected by an updated scheme in Cheng et al. (2014) modified and extended to 2023. Mechanical Bathythermograph (MBT) biases have been corrected using a newly available scheme of Gouretski and Cheng (2020). Correction for a significant systematic bias in bottle data was applied using a newly proposed correction scheme (Gouretski et al., 2022). Bias corrections for temperature profiles from sensors attached to marine animals recommended by Gouretski et al. (2023) were also applied. Together, these changes in QC procedure and bias corrections resulted in a stronger long-term upper 2000 m OHC trend for the 1960–2023 and 2005–2023 periods.

For NCEI/NOAA data, an objective analysis approach from Levitus et al. (2012) is used for spatial interpolation. The XBT biases are corrected with the Levitus et al. (2009) approach. The NCEI analysis assumes no temperature change where there is no data, which will underestimate the OHC in areas without data. However, due to Argo and other components of the ocean observing system, the coverage since 2005 is greater than 80% of the global ocean to 2000 m. Another aspect of the NCEI procedure that can lead to an underestimation of OHC is the flagging of Argo profiles in mesoscale eddies and other oceanic features, which in recent years are more than five standard deviations from the long-term (1955–2006) mean for the geographic area in which they are encountered, and thus flagged as outliers and not incorporated into the global OHC integral calculation (Tan et al., 2023). While steps are being taken to amend the QC steps to account for the features of a warming ocean, the NCEI estimates presented here do not fully represent these features in the global integral. The consequence is that the NCEI estimates are thus inherently conservative.

An additional reanalysis dataset (Escudier et al., 2021; Nigam et al., 2021) (CMS-MEDREA) is used to assess the Mediterranean changes. CMS-MEDREA assimilated XBT, CTD, and Argo profiles, integrating data from CMS and Sea-

DataNet (https://www.seadatanet.org/) and CMS satellite along-track sea level anomalies (Escudier et al., 2021). This product is generated by a numerical system composed of a hydrodynamic model supplied by the Nucleus for European Modelling of the Ocean and a variational data assimilation scheme. The model horizontal grid resolution is (1°/24°) (about 4–5 km), with 141 unevenly spaced vertical levels.

The 0–2000 m SC index (Cheng et al., 2020) is calculated for each month (t) over the 3D (x, y, z) ocean salinity field as follows:

$$\text{SC}(t) = \frac{\iiint_{V_{\text{high}}} S(x,y,z,t)\,dV}{\iiint_{V_{\text{high}}} dV} - \frac{\iiint_{V_{\text{low}}} S(x,y,z,t)\,dV}{\iiint_{V_{\text{low}}} dV} \,,$$

where (x, y, z) are latitude, longitude, and depth; V_{high} is the salinity averaged where salinity is higher than the climatological global median S_{clim}; and V_{low} is the salinity averaged where salinity is lower than the climatological global median S_{clim}. S_{clim}, V_{high} and V_{low} are determined based on the climatological salinity field during 1960–2017. The IAP/CAS data are used to calculate the SC index.

Ocean stratification is calculated (Li et al., 2020a) as the squared buoyancy frequency (N^2):

$$N^2 = gE = g\left[-\left(\frac{1}{\rho}\right)\left(\frac{\partial \sigma_n}{\partial z}\right)\right],$$

where ρ, σ_n, and g denote the sea water density, local potential density anomaly, and gravitational acceleration, respectively. The quantity N represents the Brunt–Väisälä frequency—the intrinsic frequency of internal waves.

The spatial inhomogeneity index defines the spatial spreads of water mass property A, such as temperature T (Ren et al., 2022), calculated as its volume-weighted spatial standard deviation (SSD) over the global upper 2000 m ocean as follows:

$$\text{SSD}_A(t) = \left(\frac{n}{(n-1)\sum_{x,y,z} w(x,y,z)} \sum_{x,y,z}\left\{\left[A(x,y,z,t) - \bar{A}(t)\right]^2 \times w(x,y,z)\right\}\right)^{1/2},$$

where (x, y, z, t) represent longitude, latitude, depth, and time; w is the volume centered at a given grid point (x, y, z); n is the number of grid points in the global ocean, and $\bar{A}$ represents the volume-weighted spatially averaged value. $\text{SSD}_A = 0$ indicates that property A is spatially uniform.

3. Global ocean changes of OHC, salinity, and stratification

### 3.1. *OHC and surface temperatures*

The global upper 2000 m OHC changes since 1958 (Fig. 2) show that, regardless of the processing techniques, there has been an unequivocal ocean warming trend in recent decades. The upper 2000 m of the world's ocean has warmed on average by 6.6 ± 0.3 ZJ yr^{-1} during 1958–2023 (IAP/CAS) and by 5.4 ± 0.4 ZJ yr^{-1} during 1958–2020 (NCEI/NOAA pentadal estimate). The 95% confidence levels are calculated using the approach of Cheng et al. (2022b). However, these trends do not match within the error bars, probably because of (1) conservative assumptions by NOAA when there are no data (relax to climatology in data gaps), especially in the presence of global warming trends; and (2) the difference in XBT/MBT bias correction and the new inclusion of the bottle data bias correction (Gouretski and Cheng, 2020; Gouretski et al., 2022).

Regardless of which estimate is used, there has been a two- to three- fold increase in the rate of increase in OHC since the late 1980s. For example, according to the IAP analysis, the OHC trend for 1958–1985 is 3.1 ± 0.5 ZJ yr^{-1}, and since 1986, the OHC trend is 9.2 ± 0.5 ZJ yr^{-1} (Fig. 2). The IAP trend within 1958–1985 of 3.1 ± 0.5 ZJ yr^{-1} is higher than the previous release in Cheng et al. (2023) (2.3 ± 0.5 ZJ yr^{-1}), mainly because the new inclusion of the bottle data bias correction.

After 2007, with better global coverage of ocean subsurface data, OHC uncertainty is reduced. There is a significant warming trend of 10.8 ± 1.2 ZJ yr^{-1} and 10.3 ± 0.8 ZJ yr^{-1} from 2007–2023 for IAP/CAS and NCEI/NOAA (seasonal time series), respectively (Fig. 2). The NCEI three-month OHC estimate has a slightly stronger trend than the pentadal time series from 2005 to 2020, indicating the impact of sampling changes associated with the mapping approach.

OHC tends to peak shortly before and then decline during and after an El Niño event, associated with ocean heat release into the atmosphere, mainly through increased evaporation (Cheng et al., 2019). In 2023, OHC was at the highest level ever recorded in the world's ocean, and the El Niño effects may not yet be fully evident. The 2023 upper 2000 m OHC exceeds that of 2022 by 15 ± 10 ZJ according to IAP/CAS data, and by 9 ± 5 ZJ according to NCEI/NOAA data (for the 0–2000 m layer; 95% confidence interval is presented; Table 1). A ranked ordering of the hottest five years for global OHC is provided in Table 1. The annual OHC values from 2019 to 2022 updated in this paper (Table 1) are collectively higher (~20 ZJ) than the numbers in the previous release (Cheng et al., 2023), because of the update of the IAP/CAS dataset that led to higher OHC anomalies after 2019 relative to the 1981–2010 baseline. Preliminary analyses suggest the difference is likely attributed to the replacement of the WOD-QC system (used in previous IAP analyses) by the new CODC-QC systems. Tan et al. (2023) indicated that the WOD-QC system has removed more positive anomalies than CODC-QC. The bias corrections to data collected by marine animals play a secondary role. The difference in 2023 OHC values between the two groups is also primarily attributed to the data QC, which relates to how the outliers are defined and flagged with a secondary contribution from the mapping approach. A careful investigation is warranted to reconcile the two groups' estimates.
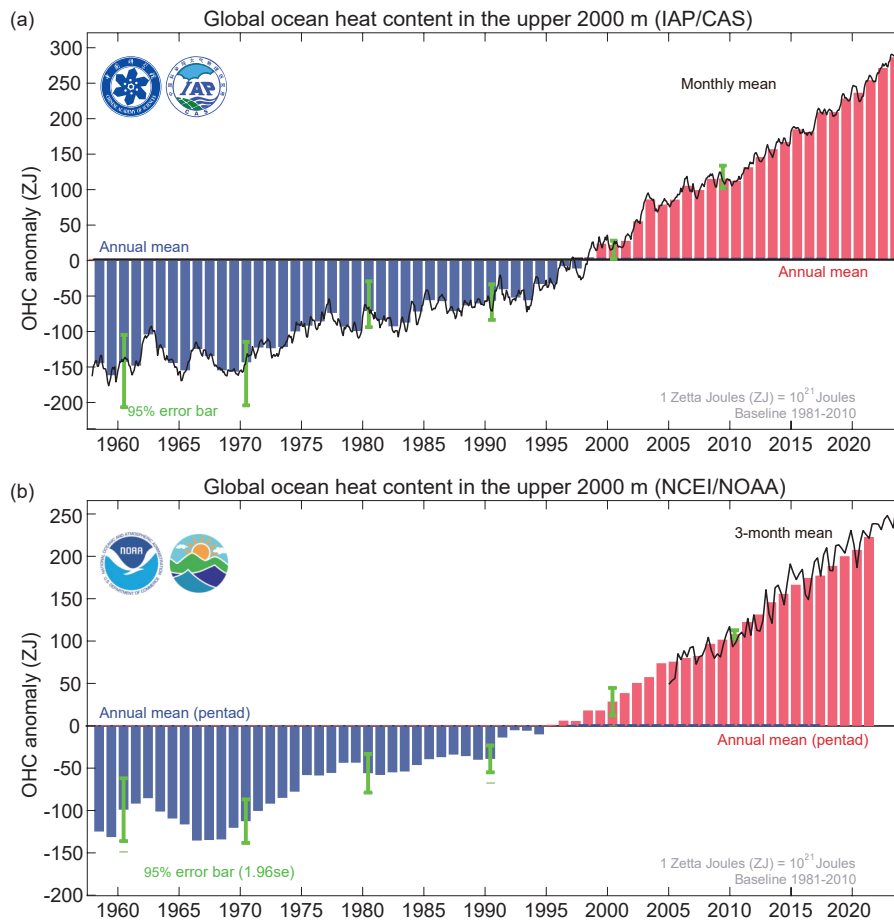
Fig. 2. Global upper 2000 m OHC from 1958 through 2023 according to (a) IAP/CAS and (b) NCEI/NOAA (1 ZJ = 10^{21} J). The line shows (a) monthly and (b) seasonal values, and the histogram presents (a) annual and (b) pentad anomalies relative to a 1981–2010 baseline.

Table 1. Ranked order of the five hottest years of the world's ocean since 1955. The OHC values are for the upper 2000 m in units of ZJ. The SST values are in °C. Both OHC and SST anomalies are relative to the 1981–2010 average. Note the IAP/CAS values are collectively higher (~20 ZJ) than the previous release (Cheng et al., 2023) because of the update of the IAP/CAS dataset that led to higher OHC anomalies relative to the 1981–2010 baseline.

Rank	Year	OHC (IAP/CAS) (units: ZJ)	OHC (NCEI/NOAA) (units: ZJ)	SST anomaly (IAP/CAS) (units: °C)
1	2023	286	247	0.54
2	2022	271	238	0.31
3	2021	254	229	0.28
4	2020	237	211	0.38
5	2019	228	210	0.40

During an El Niño event, there is a heat redistribution from the 100–500 m layer into the upper ~100 m layer, yielding higher SST than normal (Cheng et al., 2019). The anomalously high SST leads to a higher global mean surface temperature (GMST) (Trenberth et al. 2002; Li et al., 2024). In 2023, the SST became the highest on record after April, and the annual mean was 0.23°C higher than in 2022 and an astounding 0.54°C higher than the 1981–2020 average (Fig. 3). By June 2023, global monthly SSTs were already ~0.2°C above those of any prior year, an exceedingly large value (Fig. 3) that also meant GMSTs were the highest on

record. The monthly SST anomaly in 2023 relative to 1981–2010 grew from 0.35°C in January to 0.67°C in September, making September 2023 the hottest month on record for global SSTs. Normally, the hottest month for SST in a particular year occurs in March, at the end of the southern summer, because there is a large ocean area in the Southern Hemisphere (Fig. 3 inner box plot). Although SST has increased dramatically in 2023, the OHC increase has been steady over time (Fig. 2). Therefore, it is the relatively small year-to-year natural variability in OHC relative to the warming trend that makes OHC such a good indicator of climate

Global mean sea surface temperature (SST) change
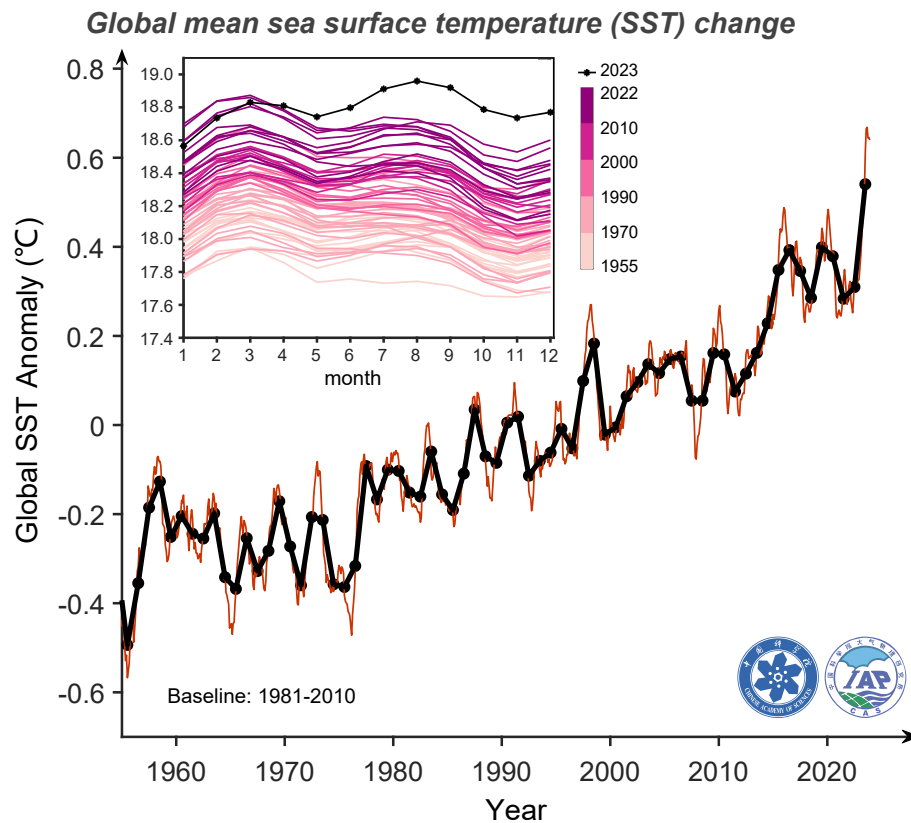
Fig. 3. Global SST changes from 1955 through 2023 according to first level (1 m) data in the IAP/CAS temperature gridded analysis (°C). The black line is the annual value, and the red is the monthly value. The anomalies are relative to a 1981–2010 baseline. The within-year variation of SST is shown in the inner box, with 2023 values shown in black.

change.

3.2. *Other oceanic climate indicators*

Substantial changes are also seen in other oceanic metrics. The upper 2000 m SC index time series since 1958 (Fig. 4) reveal a robust increase in the SC index in the past half-century, indicating an amplification of the 0–2000 m salinity pattern (Cheng et al., 2020). The SC index reached 7.2 mg kg^{-1} in 2023, the fourth-highest value since 1958. However, the difference between the top 5 years 2017, 2022, 2021, 2023, and 2019) is not statistically significant because of the large inter-annual variability and data uncertainty; for instance, there are more real-time Argo salinity data recently that have not undergone careful quality-control and bias adjustment. This ocean-based metric is generally consistent with many atmosphere-based estimates and strengthens the evidence that the global water cycle has been amplified with global warming (Cheng et al., 2020). On land, the amplified water cycle means stronger and longer dry spells and more heavy rainfall events with the potential for flooding, as observed (Fischer et al., 2021).

Ocean density stratification has also increased since the late 1950s (Fig. 4b) because of the change in vertical temperature and salinity structure (Li et al., 2020a). The stratification index shows stronger interannual to decadal variability than

the OHC and SC-index because it reveals more upper-ocean changes, which shows stronger anomalies than the deeper ocean. In 2023, the upper 2000 m stratification increased to $(6.93 \pm 0.39) \times 10^{-7}$ s^{-2}, reaching record high values in 2023 mainly because of the development of the strong El Niño.

The spatial inhomogeneity index of ocean temperature has also increased since the 1950s (Fig. 4c), with a trend of 0.020 ± 0.003°C $(10 \text{ yr})^{-1}$. This index reached a record high of 0.093°C in 2023 relative to a 1981–2010 baseline, indicating a substantial increase in ocean temperature spatial variance. The non-uniform upper-ocean warming, which was more rapid at mid-to-low latitudes, was mainly responsible for this index increase in 2023 (Ren et al., 2022).

4. Regional patterns of ocean warming and salinity

Spatial maps of the 2022 OHC anomaly relative to the mean 1981–2010 conditions (Fig. 5) reveal that most of the ocean areas are warming significantly, while some areas (much of the Atlantic, North Pacific, Western Pacific, and southern oceans) are heating at a faster rate than the global average (0.8 GJ m^{-2} yr^{-1}, 1 GJ = 10^9 J). The drivers of the long-term OHC trend patterns were discussed
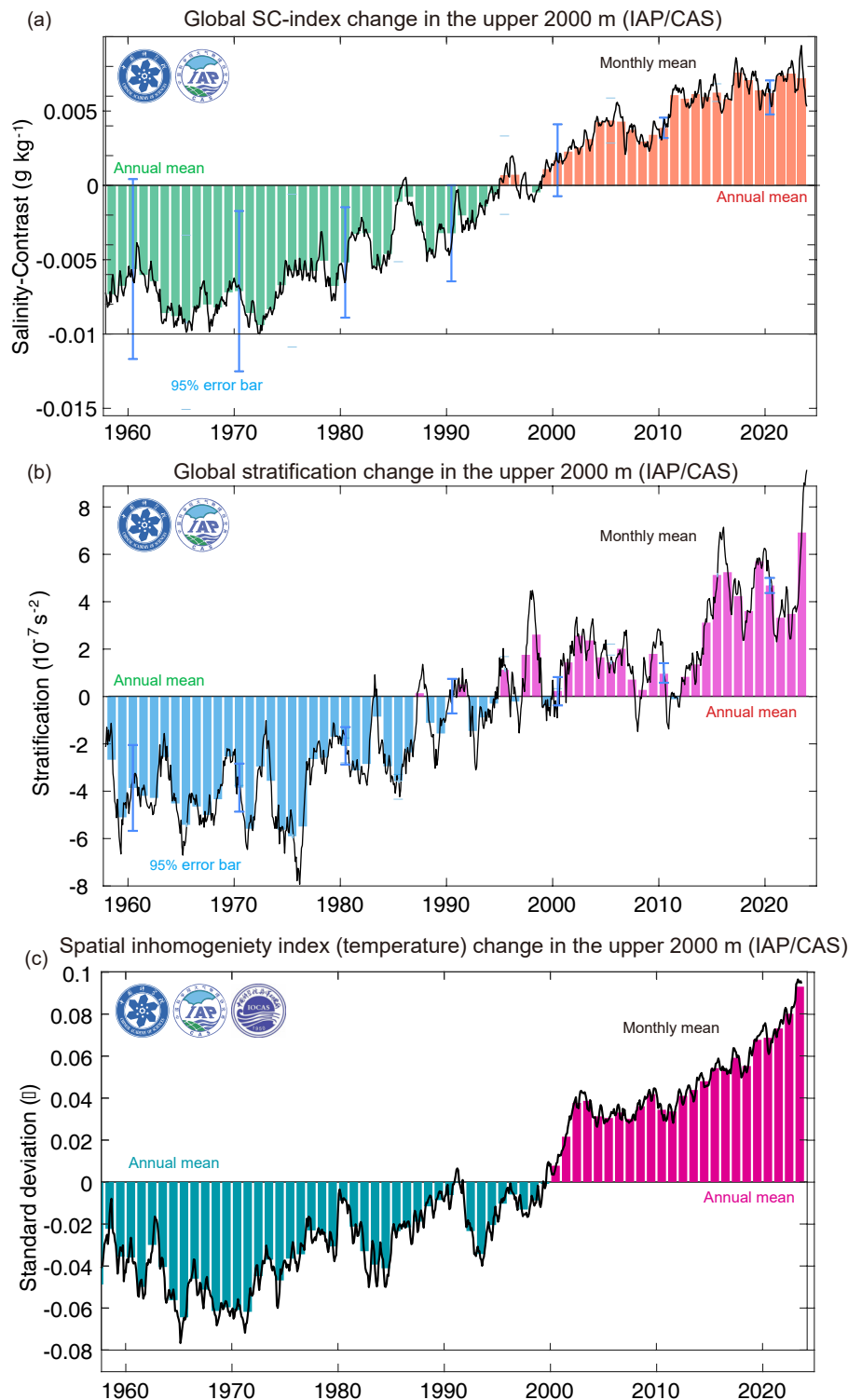
Fig. 4. Monthly (black line) and annual (color bars) changes in (a) SC index, (b) stratification, and (c) spatial inhomogeneity index of temperature in the upper 2000 m of the global ocean from 1958 to 2023 [data updated from Cheng et al. (2017)]. The units for salinity are g kg^{-1} (using absolute salinity).

by Cheng et al. (2022a, c).

　　The OHC annual mean difference between 2023 and 2022 is presented in Fig. 6. In the tropical Pacific, strong warming anomalies in the eastern Pacific and cooling anoma-

lies in the western Pacific in 2023 (Fig. 6) indicate the shoaling of the equatorial thermocline associated with El Niño. The zonal OHC shows strong tropical warming within 8°S–3°N, which is partly offset by the cooling around 5°N and

2023 OHC (0-2000m) anomaly relative to 1981-2010 baseline (IAP/CAS)
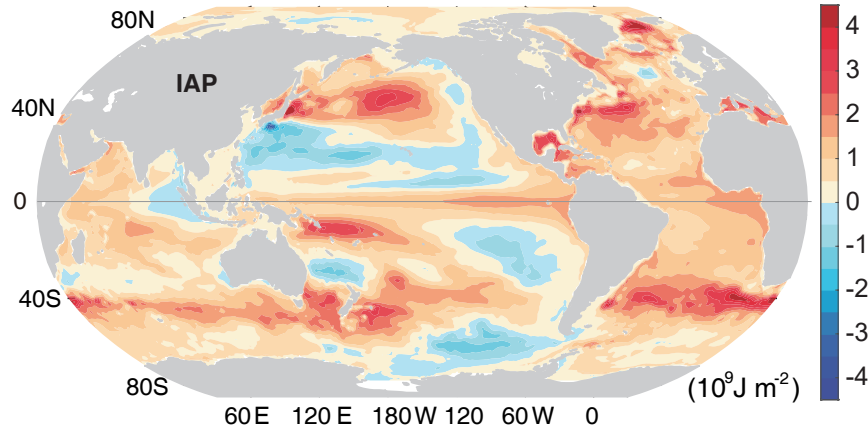
Fig. 5. The annual OHC anomaly in 2023 relative to a 1981–2010 baseline for IAP/CAS data; units: 10^9 J m^{-2} [data updated from Cheng et al. (2017)].
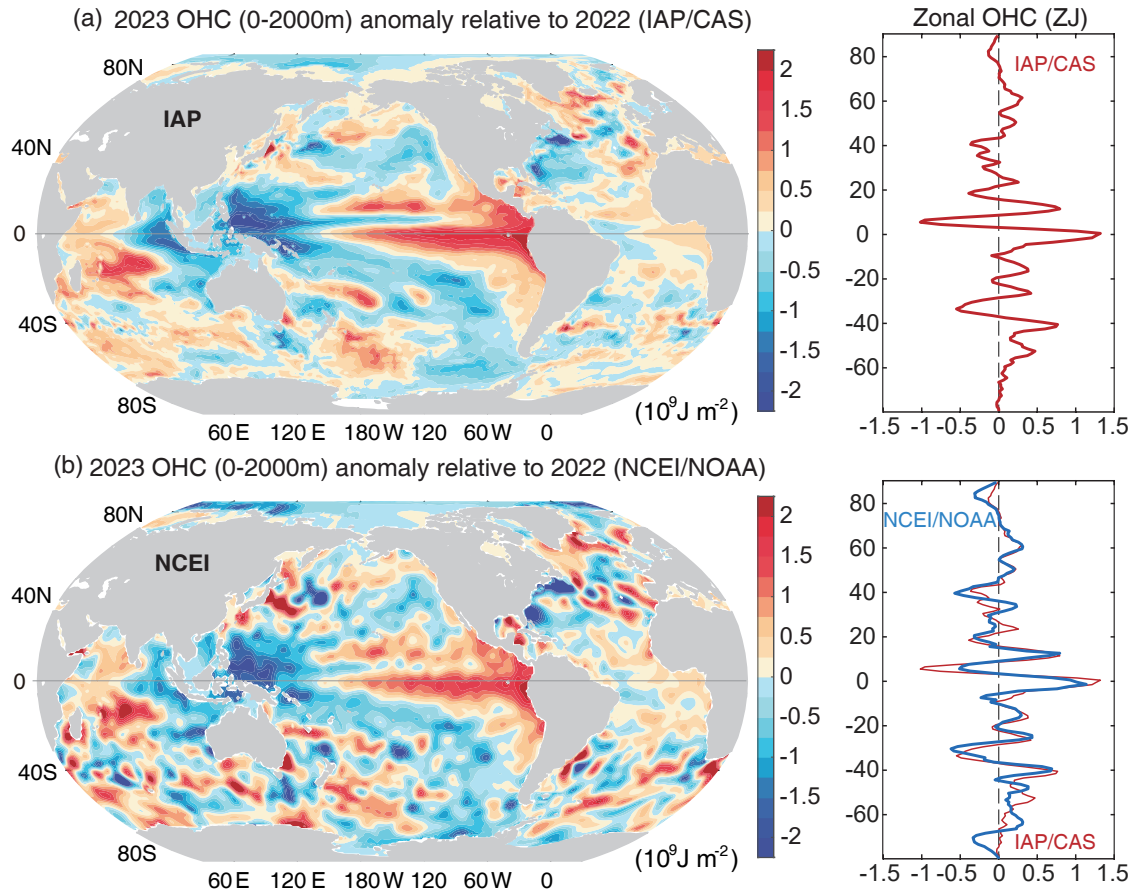
Fig. 6. (a) Differences of annual mean upper 2000 m OHC values between 2023 and 2022, based on IAP/CAS analysis. (b) As in (a) but for the NCEI/NOAA analysis. Units: 10^9 J m^{-2}. The zonal OHCs are presented on the right-hand side of the spatial maps [data updated from Cheng et al. (2017) in (a), and from Levitus et al. (2012) in (b)].

8°S. The two estimates show consistent large-scale patterns, but the NCEI/NOAA data are noisier, mainly because of the mapping approach.

The 2023 salinity anomalies relative to a 1981–2010 baseline (Fig. 7a) reveal freshening trends for most of the Pacific and Indian oceans, with relatively saline areas such

as the midlatitude Atlantic, the Mediterranean Sea, and the West Indian Ocean becoming more saline. This is a typical "fresh gets fresher, salty gets saltier" pattern change driven by atmospheric hydrological cycle amplification. The tropical salinity changes reveal more of the impact of El Niño, especially in the western Pacific and around the Intertropical Con-
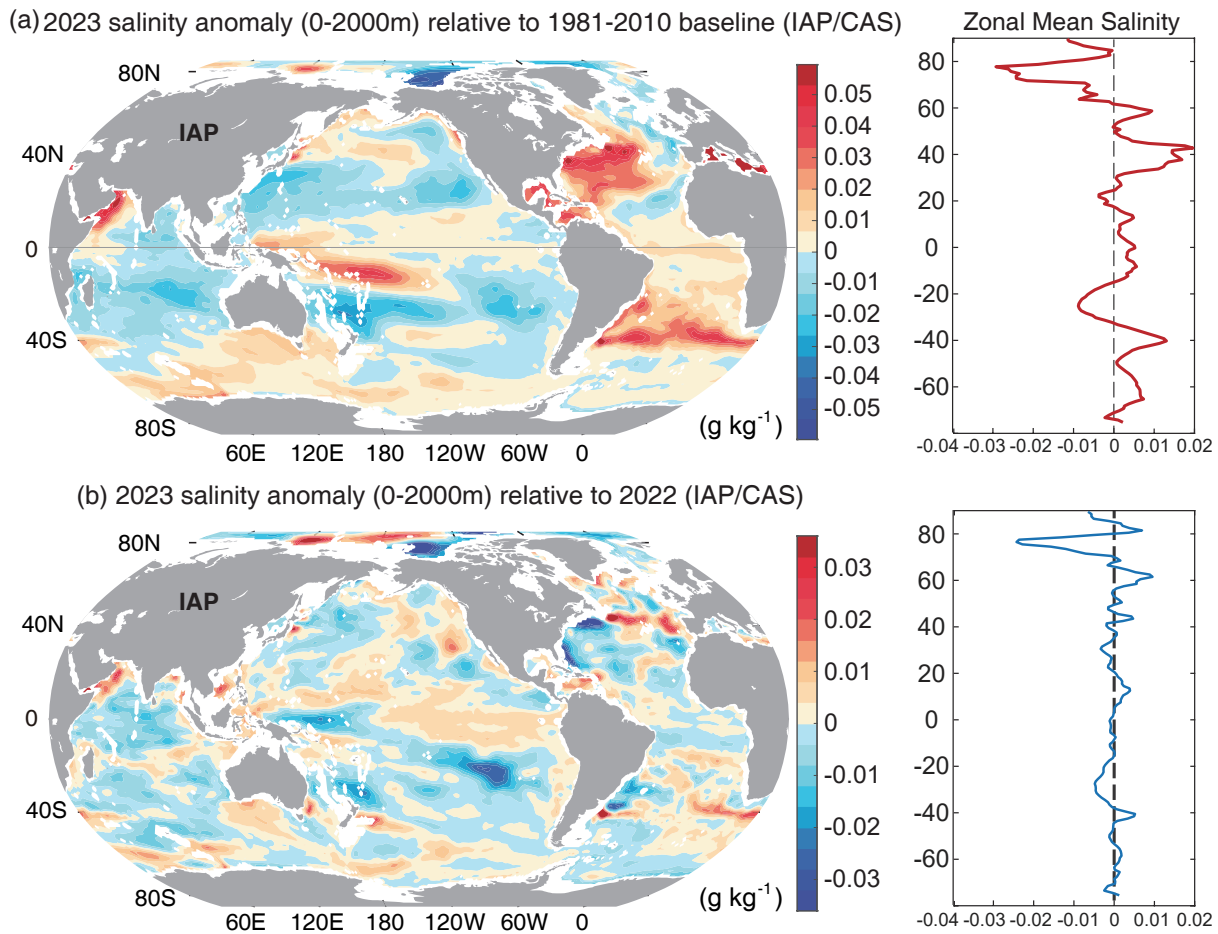
Fig. 7. (a) The upper 2000 m salinity anomaly in 2023 relative to a 1981–2010 baseline. (b) The difference in salinity in the upper 2000 m between 2023 and 2022. The zonal mean salinity anomalies are presented on the right-hand side of the spatial maps [data updated from Cheng et al. (2020)].

vergence Zone (ITCZ) (5°–10°N). During the El Niño event, the upward branch of the Walker circulation moves into the tropical central Pacific Ocean, resulting in less rainfall in the western Pacific and ITCZ and an increase in ocean salinity (Fig. 7b).

5. Basin-wide OHC changes and regional hotspots

The evolution of regional OHC in seven ocean regions is presented in Fig. 8 for 1958 to 2023. The northwest region of the Pacific Ocean, bounded by ~10°S–30°N and ~110°–170°E, is dominated by substantial interannual and decadal internal variability, especially from the Interdecadal Pacific Variability and ENSO (OHC is higher during the La Niña year). Since 2000, the upper 2000 m OHC values have collectively been higher than in 1958–2000. In 2023, the Northwest Pacific OHC is lower than in 2020–22 because of El Niño (Fig. 8a; 0.20 GJ m⁻² above a 1981–2010 base-line, ranked 20 since 1958).

The Indian OHC in 2023 is among the top five record years (Fig. 8b; 0.71 GJ m⁻² relative to a 1981-2010 base-line). The decrease in OHC from 2020 to 2022 is consistent with the negative Indian OHC tendency during La Niña (Cheng et al., 2019), driven mainly by decreasing the heat transport through the Indonesian Throughflow passages dur-ing the decaying stage of La Niña (Trenberth and Zhang, 2019; Li et al., 2020b; Volkov et al., 2020). However, the Indian OHC has shown a continuous increase since January 2023, associated with the cessation of La Nina and the devel-opment of El Niño.

The tropical Atlantic Ocean (10°–30°N), a region impor-tant for hurricane development (Trenberth et al., 2018), shows a continual increase in OHC since the late 1950s (Fig. 8c). The upper 2000 m OHC in 2023 reached the highest value ever recorded (1.24 GJ m⁻² in 2023 higher than the 1981–2010 baseline, and it is 0.07 GJ m⁻² higher than 2022).

In the North Atlantic Ocean, the upper 2000m OHC was near its record high in 2023, lower than 2022 by 0.01 GJ m⁻² and lower than 2021 by 0.04 GJ m⁻². Although El Niño years tend to have slightly weaker hurricane sea-sons, the Atlantic basin saw 20 named storms in 2023 (includ-ing seven hurricanes), which ranks fourth for the number of storms in a year since 1950 (https://www.noaa.gov/news-release/2023-atlantic-hurricane-season-ranks-4th-for-most-
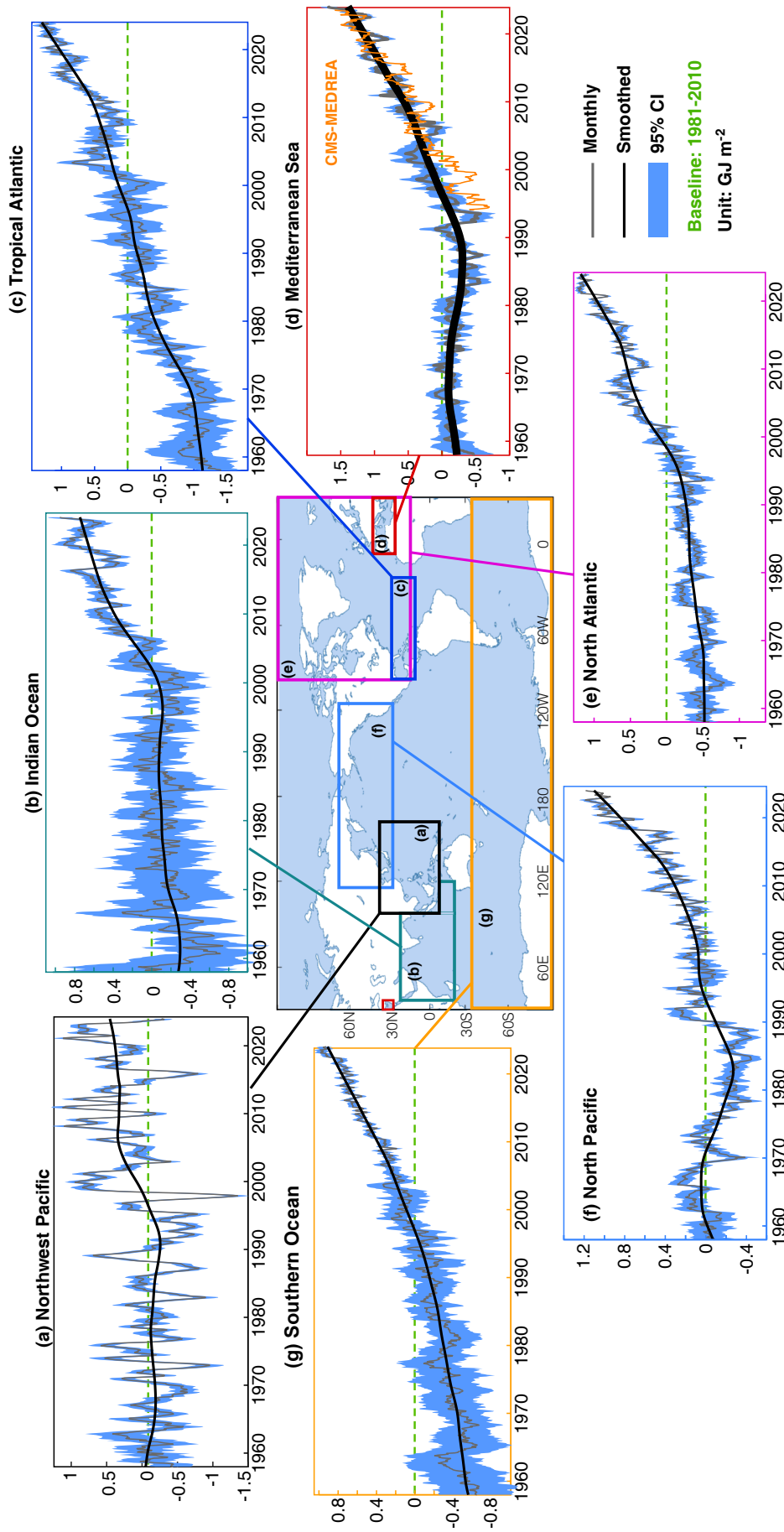
Fig. 8. Regional observed upper 2000 m OHC change from 1958 through 2023 relative to a 1981–2010 baseline. The time series (black lines) are smoothed by LOWESS (locally weighted scatterplot smoothing) with a span width of 240 months. The gray shaded areas are the 95% confidence intervals [data updated from Cheng et al. (2017)].

named-storms-in-year). In 2023, the SST in the North Atlantic Ocean has been at a record high since March. The maximum temperature is > 1°C higher than the 1981–2010 average. These warm anomalies are mainly distributed in the eastern North Atlantic Ocean and are shallow, being confined to the upper 100 m ocean (Fig. 9). The causes of these anomalies remain a topic of investigation.

In the North Pacific Ocean (30°–62°N), an area of large-scale warming (> 2°C) and marine heatwaves [named "The Blob" (Scannell et al., 2020)] persisted in 2023 (Figs. 5, 6 and 8). The upper 2000 m OHC has decreased slightly by 0.03 GJ m^{-2} compared with 2022. The upper 2000 m OHC in the Southern Ocean in 2023 exceeded the 2022 value by 0.09 GJ m^{-2} (Fig. 8g), continuing its long-term increasing trend since the 1960s.

The Mediterranean Sea OHC in 2023 was higher than in 2022 by 0.31 GJ m^{-2} (Fig. 8d) for IAP/CAS data and by 0.23 GJ m^{-2} for independent ocean reanalysis data (CMS-MEDREA; Escudier et al., 2021; Nigam et al., 2021), indicating a record-high OHC in 2023 (Fig. 8d). A marked temperature increase has been measured in the last few decades in the Mediterranean Sea, starting from the Eastern Basin where warmer (and saltier) Intermediate Waters formed and spread towards the Western Basin on their way back to the North Atlantic (Pinardi et al., 2015; Von Schuckmann et al., 2016; Simoncelli et al., 2018). Accurate measurements provided by a CNR_ISMAR mooring in the Sicily Channel since 1993 (Schroeder et al., 2017; Ben Ismail et al., 2021; available at https://doi.org/10.48670/moi-00044) and the temperatures resulting from the monitoring with XBT probes in the Tyrrhenian and Ligurian Seas since 1999 along the MX04 Genoa-Palermo line (Reseghetti et al., 2023; Simon-

celli et al., 2023) (Fig. 10a), indicated clear warming in the 150–450 m layer that started in spring 2013 (Cheng et al., 2022c). This warming region subsequently extended deeper and northward, reaching 700 m in 2016 (Fig. 10b). Data from MX04 and from the Sicilian Channel mooring indicate warming in the period 2013–16 above 0.4°C (Fig. 10c) and, after a slight decrease and a stationary period, a recovery in growth in 2021, culminating for now in September 2023 when a new maximum temperature record was measured along the MX04 line. The linear rate calculated for the period 2004–23 is 0.025°C yr^{-1} for the MX04 area, while it is 0.027°C yr^{-1} in the Sicily Channel.

6. Concluding remarks

Based on analyses conducted by several independent research groups, this paper provides updates of the SST, OHC, salinity, stratification, and a spatial temperature inhomogeneity index for the year 2023. The ocean continued to warm globally in 2023, not only at the surface but also across the upper 2000 m. The warming rate has increased in recent decades, with a faster rate of warming evident since around 1990 (Cheng et al., 2022a, b). Similarly, the SC index has increased, signifying more extreme salinity anomalies and an imprint of global water cycle amplification on the upper ocean. Ocean stratification also was at a record high in 2023, with upper ocean waters becoming more stable over time, although with more variability than other climate characteristics. Regional warming patterns reveal that three out of seven investigated regions in this study reached record levels of their upper 2000 m OHC in 2023.

Given the disparities between IAP/CAS and NOAA/
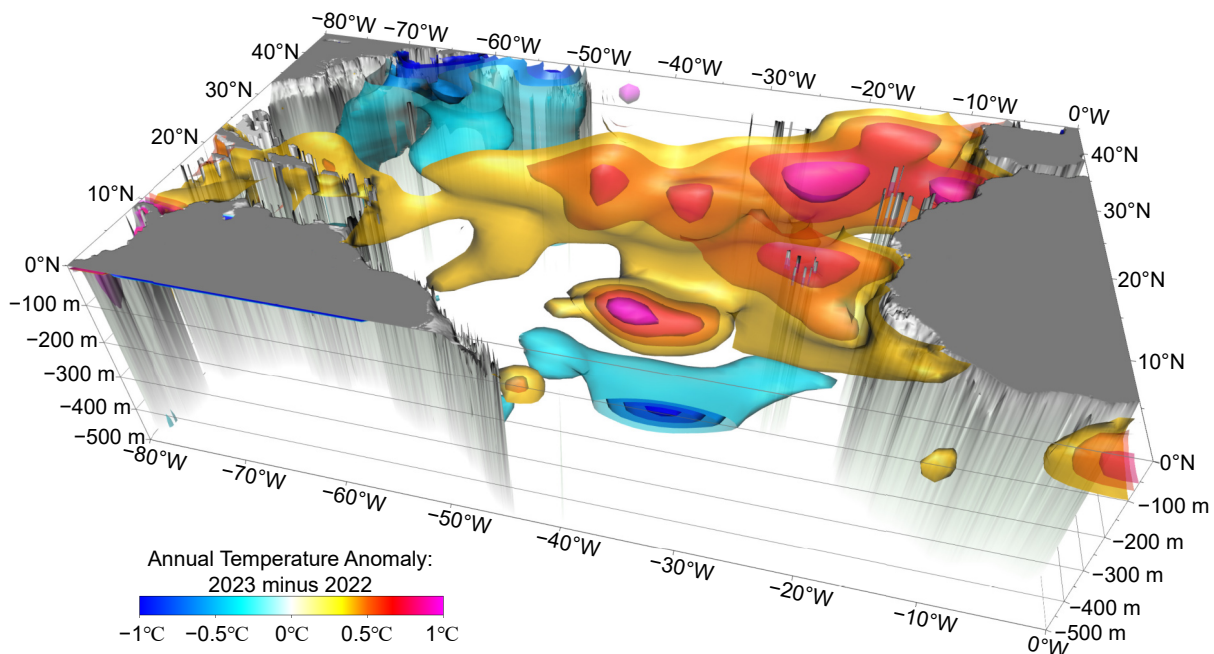
Fig. 9. Three-dimensional fields of oceanic temperature changes in 2023 relative to 2022 in the North Atlantic Ocean. The NCEI/NOAA data are used, and the illustration is modified with domains and angles from Seidov et al. (2021).
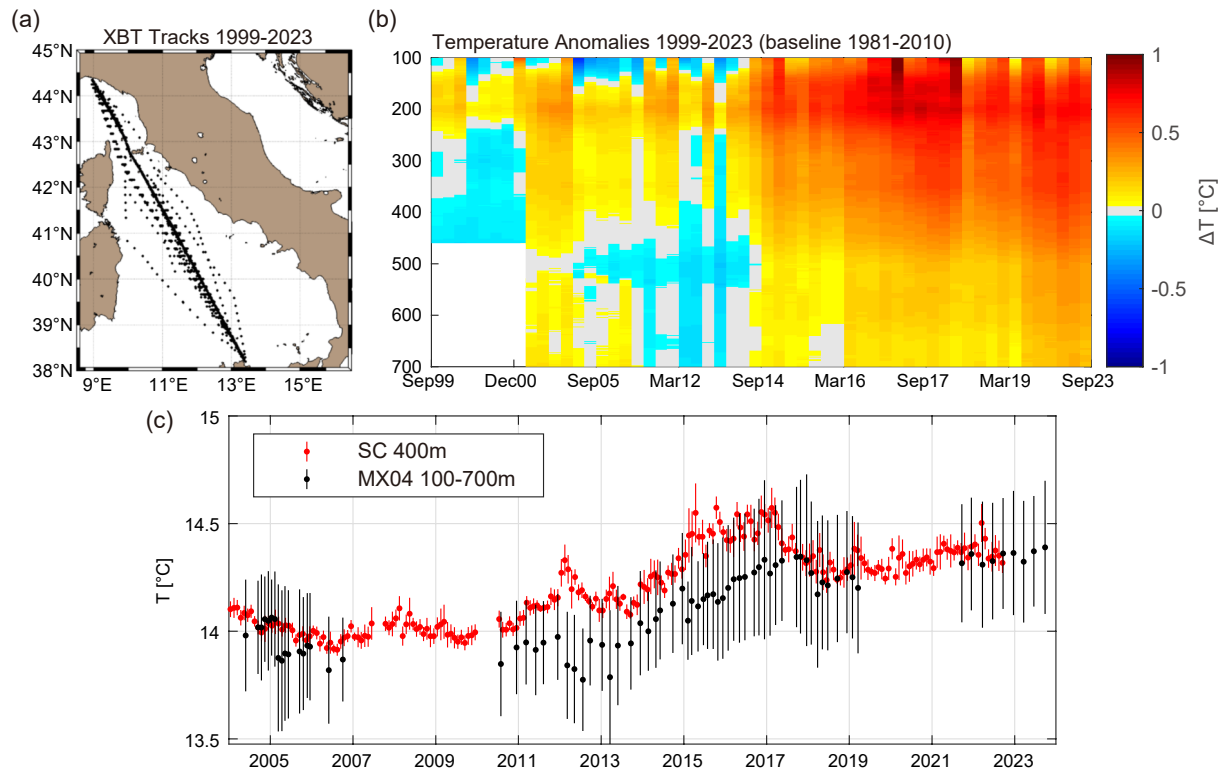
Fig. 10. Temperature along the MX04 Genova–Palermo transect (western Mediterranean) recorded by XBT probes from ships of opportunity and monthly mean temperature values at 400 m from the Sicily Channel mooring. (a) XBT tracks in the Tyrrhenian and Ligurian seas. (b) Hovmöller plot of mean MX04 temperature anomalies in 1999–2023 computed by subtracting the 1981–2010 baseline of IAP/CAS data. (c) MX04 mean temperature values computed in the layers of 100–700 m, and monthly mean temperature values at 400 m from the Sicily Channel mooring, between 2004 and 2023, with the error bars representing the relative standard deviations. The standard deviations associated with the two time-series differ by one order of magnitude owing to the variability associated with the daily temperature sampled at a single location (400 m deep) or the daily temperature within a specific layer (100–700 m) sampled along a line, about 430 nautical miles long.

NCEI OHC change estimates between 2023 and 2022 (15 ZJ for IAP/CAS and 9 ZJ for NOAA/NCEI), a further bulk check was attempted. The CERES 2023 January–October mean net EEI anomaly is 1.88 W m^{-2}, although values were decreasing sharply in late 2023. Assuming zero for November and December, the CERES 2023 anomaly would be 1.57 W m^{-2} for the year or 25 ZJ. Further, if 90% of this went into the ocean, the OHC increase would be 22.5 ZJ. For global sea level (https://sealevel.colorado.edu/data/2023rel2), the estimated change between January–October 2023 and January–December 2022 is 5.58 mm. Converting SLR to the contribution from OHC depends critically on where the heat is added. Firstly, SLR is usually dominated by volume and mass changes from melting land ice, and a reasonable estimate is that ocean warming contributes 2.5 mm from expansion. The SL response varies a lot depending on where heat is deposited (Fasullo et al., 2020); the response is greater for higher temperatures, and a rough estimate is that the required heat added is 20–30 ZJ. Hence, even though these bulk global estimates vary, they show the way forward for reducing uncertainty, and all indicate substantial warming in 2023.

REFERENCES

Abraham, J., and Coauthors, 2013: A review of global ocean tem-perature observations: Implications for ocean heat content esti-mates and climate change. *Rev. Geophys.*, **51**, 450–483, https://doi.org/10.1002/rog.20022.

Abraham, J., L. J. Cheng, M. E. Mann, K. Trenberth, and K. Von Schuckmann, 2022: The ocean response to climate change guides both adaptation and mitigation efforts. *Atmos. Ocean. Sci. Lett.*, **15**, 100221, https://doi.org/10.1016/j.aosl.2022.100221.

Abraham, J. P., and L. J. Cheng, 2022: Intersection of climate change, energy, and adaptation. *Energies*, **15**, 5886, https://doi.org/10.3390/en15165886.

Argo, 2023: Argo Float Data and Metadata from Global Data Assembly Centre (Argo GDAC). SEANOE. Available from https://doi.org/10.17882/42182.

Ben Ismail S., K. Schroeder, J. Chiggiato, S. Sparnocchia, and M. Borghini, 2021: Long term changes monitored in two Mediter-ranean Channels. *Copernicus Marine Service Ocean State Report, Issue 5*, K. Von Schuckmann et al., Eds., 48–52, https://doi.org/10.1080/1755876X.2021.1946240.

Boyer, T., and Coauthors, 2016: Sensitivity of global upper-ocean heat content estimates to mapping methods, XBT bias corrections, and baseline climatologies. *J. Climate*, **29**, 4817–4842, https://doi.org/10.1175/JCLI-D-15-0801.1.

Boyer, T. P., and Coauthors, 2018: World ocean database 2018. NOAA Atlas NESDIS 87.

Cheng, L. J., J. Zhu, R. Cowley, T. Boyer, and S. Wijffels, 2014: Time, probe type, and temperature variable bias corrections to historical expendable bathythermograph observations. *J. Atmos. Oceanic Technol.*, **31**(8), 1793–1825, https://doi.org/10.1175/JTECH-D-13-00197.1.

Cheng, L. J., K. E. Trenberth, J. Fasullo, T. Boyer, J. Abraham, and J. Zhu, 2017: Improved estimates of ocean heat content from 1960 to 2015. *Science Advances*, **3**, e1601545, https://doi.org/10.1126/sciadv.1601545.

Cheng, L. J., K. Trenberth, J. Fasullo, J. Abraham, T. Boyer, K. Von Schuckmann, and J. Zhu, 2018: Taking the pulse of the planet. *Eos*, **99**, 14–16, https://doi.org/10.1029/2017EO081839.

Cheng, L. J., K. E. Trenberth, J. T. Fasullo, M. Mayer, M. Bal-maseda, and J. Zhu, 2019: Evolution of ocean heat content related to ENSO. *J. Climate*, **32**, 3529–3556, https://doi.org/10.1175/JCLI-D-18-0607.1.

Cheng, L. J., and Coauthors, 2020: Improved estimates of changes in upper ocean salinity and the hydrological cycle. *J. Climate*, **33**, 10 357–10 381, https://doi.org/10.1175/JCLI-D-20-0366.1.

Cheng, L. J., and Coauthors, 2022a: Past and future ocean warm-ing. *Nature Reviews Earth & Environment*, **3**, 776–794, https://doi.org/10.1038/s43017-022-00345-1.

Cheng, L. J., G. Foster, Z. Hausfather, K. E. Trenberth, and J. Abra-ham, 2022b: Improved quantification of the rate of ocean warming. *J. Climate*, **35**, 4827–4840, https://doi.org/10.1175/JCLI-D-21-0895.1.

Cheng, L. J, and Coauthors, 2022c: Another record: Ocean warm-ing continues through 2021 despite La Niña conditions. *Adv. Atmos. Sci.*, **39**(3), 373–385, https://doi.org/10.1007/s00376-022-1461-3.

Cheng, L. J., and Coauthors, 2023: Another year of record heat for the oceans. *Adv. Atmos. Sci*, **40**, 963–974, https://doi.org/10.1007/s00376-023-2385-2.

Durack, P. J., and S. E. Wijffels, 2010: Fifty-year trends in global ocean salinities and their relationship to broad-scale warm-ing. *J. Climate*, **23**, 4342–4362, https://doi.org/10.1175/2010JCLI3377.1.

Escudier, R., and Coauthors, 2021: A high resolution reanalysis for the mediterranean sea. *Front. Earth Sci.*, **9**, 702285, https://doi.org/10.3389/feart.2021.702285.

Fischer, E. M., S. Sippel, and R. Knutti, 2021: Increasing probabil-ity of record-shattering climate extremes. *Nature Climate Change*, **11**, 689–695, https://doi.org/10.1038/s41558-021-01092-9.

Fasullo, J. T., Gent, P. R., and Nerem, R. S. 2020: Forced patterns of sea level rise in the community earth system model large ensemble from 1920 to 2100. *Journal of Geophysical Research: Oceans*, 125, e2019JC016030. https://doi.org/10.1029/2019JC016030

Gouretski, V., and L. J. Cheng, 2020: Correction for systematic errors in the global dataset of temperature profiles from mechanical bathythermographs. *J. Atmos. Oceanic Technol.*, **37**(5), 841–855, https://doi.org/10.1175/JTECH-D-19-0205.1.

Gouretski, V., L. J. Cheng, and T. Boyer, 2022: On the consistency of the bottle and CTD profile data. *J. Atmos. Oceanic Tech-nol.*, **39**(12), 1869–1887, https://doi.org/10.1175/JTECH-D-22-0004.1.

Gouretski, V., F. Roquet, and L. J. Cheng, 2023: Measurement biases in ocean temperature profiles from marine mammal data loggers. *J. Atmos. Oceanic Technol.*, submitted.

Gulev, S., and Coauthors, 2021: Changing state of the climate sys-

tem. *Climate Change 2021: The Physical Science Basis. Contribution of Working Group I to the Sixth Assessment Report of the Intergovernmental Panel on Climate Change*, V. Masson-Delmotte et al., Eds., Cambridge University Press.

Huang, B. Y., and Coauthors, 2017: Extended reconstructed sea surface temperature, Version 5 (ERSSTv5): Upgrades, validations, and intercomparisons. *J. Climate*, **30**, 8179−8205, https://doi.org/10.1175/JCLI-D-16-0836.1.

Johnson, G., and Coauthors, 2018: Ocean heat content [in State of the Climate in 2017]. *Bull. Amer. Meteor. Soc.*, **99**, S72−S77.

Levitus, S., J. I. Antonov, T. P. Boyer, R. A. Locarnini, H. E. Garcia, and A. V. Mishonov, 2009: Global ocean heat content 1955−2008 in light of recently revealed instrumentation problems. *Geophys. Res. Lett.*, **36**, L07608, https://doi.org/10.1029/2008GL037155.

Levitus, S., and Coauthors, 2012: World ocean heat content and thermosteric sea level change (0−2000 m), 1955−2010. *Geophys. Res. Lett.*, **39**, L10603, https://doi.org/10.1029/2012GL051106.

Li, G. C., L. J. Cheng, J. Zhu, K. E. Trenberth, M. E. Mann, and J. P. Abraham, 2020a: Increasing ocean stratification over the past half-century. *Nature Climate Change*, **10**, 1116−1123, https://doi.org/10.1038/s41558-020-00918-2.

Li, K. X., F. Zheng, L. J. Cheng, T. Y. Zhang, and J. Zhu, 2023: Record-breaking global temperature and crises with strong El Niño in 2023−2024. *The Innovation Geoscience*, **1**(2), 100030. https://doi.org/10.59717/j.xinn-geo.2023.100030.

Li, K. X., F. Zheng, J. Zhu, and Q.-C. Zeng, 2024: El Niño and the AMO sparked the astonishingly large margin of warming in the global mean surface temperature in 2023. *Adv. Atmos. Sci.*, https://doi.org/10.1007/s00376-023-3371-4.

Li, Y. L., W. Q. Han, F. Wang, L. Zhang, and J. Duan, 2020b: Vertical structure of the upper-Indian Ocean thermal variability. *J. Climate*, **33**, 7233−7253, https://doi.org/10.1175/JCLI-D-19-0851.1.

Loeb, N. G., G. C. Johnson, T. J. Thorsen, J. M. Lyman, F. G. Rose, and S. Kato, 2021: Satellite and ocean data reveal marked increase in Earth's heating rate. *Geophys. Res. Lett.*, **48**, e2021GL093047, https://doi.org/10.1029/2021GL093047.

Loeb, N. G., and Coauthors, 2022: Evaluating twenty-year trends in Earth's energy flows from observations and reanalyses. *J. Geophys. Res. Atmos.*, **127**, e2022JD036686, https://doi.org/10.1029/2022JD036686.

Nigam, T., and Coauthors, 2021: Mediterranean Sea Physical Reanalysis INTERIM (CMEMS MED-Currents, E3R1i system) (Version 1) [Data set]. Copernicus Monitoring Environment Marine Service (CMEMS). https://doi.org/10.25423/CMCC/MEDSEA_MULTIYEAR_PHY_006_004_E3R1I.

Pinardi, N., and Coauthors, 2015: Mediterranean Sea large-scale low-frequency ocean variability and water mass formation rates from 1987 to 2007: A retrospective analysis. *Progress in Oceanography*, **132**, 318−332, https://doi.org/10.1016/j.pocean.2013.11.003.

Purkey, S., and G. C. Johnson, 2010: Warming of global abyssal and deep Southern Ocean waters between the 1990s and 2000s: Contributions to global heat and sea level rise budgets. *J. Climate*, **23**, 6336−6351, https://doi.org/10.1175/2010JCLI3682.1.

Ren, Q. P., Y.-O. Kwon, J. Y. Yang, R.-X. Huang, Y. L. Li, and F. Wang, 2022: Increasing inhomogeneity of the global

oceans. *Geophys. Res. Lett.*, **49**, e2021GL097598, https://doi.org/10.1029/2021GL097598.

Reseghetti, F., C. Fratianni, and S. Simoncelli, 2023: Reprocessed of XBT dataset in the Ligurian and Tyrrhenian seas (1999−2019). Istituto Nazionale di Geofisica e Vulcanologia (INGV). [Available online from https://doi.org/10.13127/rep_xbt_1999_2019].

Rhein, M., and Coauthors, 2013: Observations: Ocean pages. *Climate Change 2013: The Physical Science Basis. Contribution of Working Group I to the Fifth Assessment Report of the Intergovernmental Panel on Climate Change*, T. F. Stocker et al., Eds., Cambridge University Press.

Scannell, H. A., G. C. Johnson, L. Thompson, J. M. Lyman, and S. C. Riser, 2020: Subsurface evolution and persistence of marine heatwaves in the Northeast Pacific. *Geophys. Res. Lett.*, **47**, e2020GL090548, https://doi.org/10.1029/2020GL090548.

Schroeder, K., J. Chiggiato, S. A. Josey, M. Borghini, S. Aracri, and S. Sparnocchia, 2017: Rapid response to climate change in a marginal sea. *Scientific Reports*, **7**, 4065, https://doi.org/10.1038/s41598-017-04455-5.

Seidov, D., A. Mishonov, and R. Parsons, 2021: Recent warming and decadal variability of Gulf of Maine and Slope Water. *Limnology and Oceanography*, **66**, 3472−3488, https://doi.org/10.1002/lno.11892.

Simoncelli, S., N. Pinardi, C. Fratianni, C. Dubois, and G. Notarstefano, 2018: Water mass formation processes in the Mediterranean Sea over the past 30 years. *In: Copernicus Marine Service Ocean State Report, Issue 2, Journal of Operational Oceanography, 11:sup1, s13−s16*, https://doi.org/10.1080/1755876X.2018.1489208.

Simoncelli, S., Reseghetti, F., Fratianni, C., Cheng, L., and Raiteri, G., 2023: Reprocessing of XBT profiles from the Ligurian and Tyrrhenian seas over the time period 1999–2019 with full metadata upgrade, *Earth Syst. Sci. Data Discuss*. [preprint], https://doi.org/10.5194/essd-2023-525, in review.

Tan, Z. T., L. J. Cheng, V. Gouretski, B. Zhang, Y. J. Wang, F. C. Li, Z. H. Liu, and J. Zhu, 2023: A new automatic quality control system for ocean profile observations and impact on ocean warming estimate. *Deep-Sea Res. Part I Oceanogr. Res. Pap.*, **194**, 103961, https://doi.org/10.1016/j.dsr.2022.103961.

Trenberth, K. E., J. T. Fasullo, and M. A. Balmaseda, 2014: Earth's energy imbalance. *J. Climate*, **27**, 3129−3144, https://doi.org/10.1175/JCLI-D-13-00294.1.

Trenberth, K. E., J. M. Caron, D. P. Stepaniak, and S. Worley, 2002: Evolution of El Niño–Southern Oscillation and global atmospheric surface temperatures. *J. Geophys. Res.*, **107,** AAC 5-1-AAC 5-17, doi: 10.1029/2000JD000298.

Trenberth, K. E., L. J. Cheng, P. Jacobs, Y. X. Zhang, and J. Fasullo, 2018: Hurricane Harvey links to ocean heat content and climate change adaptation. *Earth's Future*, **6**, 730−744, https://doi.org/10.1029/2018EF000825.

Trenberth, K. E., and Y. X. Zhang, 2019: Observed interhemispheric meridional heat transports and the role of the Indonesian Throughflow in the Pacific Ocean. *J. Climate*, **32**, 8523−8536, https://doi.org/10.1175/JCLI-D-19-0465.1.

Volkov, D. L., S.-K. Lee, A. L. Gordon, and M. Rudko, 2020: Unprecedented reduction and quick recovery of the South Indian Ocean heat content and sea level in 2014–2018. *Science Advances*, **6**, eabc1151, https://doi.org/10.1126/sciadv.abc1151.

Von Schuckmann, K., and Coauthors, 2016: The Copernicus marine environment monitoring service ocean state report. *Journal of Operational Oceanography*, **9**, s235−s320, https://doi.org/10.1080/1755876X.2016.1273446.

Von Schuckmann, K., and Coauthors, 2020: Heat stored in the Earth system: Where does the energy go? *Earth System Science Data*, **12**, 2013−2041, https://doi.org/10.5194/essd-12-2013-2020.

Zheng, F., and J. Zhu, 2016: Improved ensemble-mean forecasting of ENSO events by a zero-mean stochastic error model of an intermediate coupled model. *Climate Dyn.*, **47**, 3901−3915, https://doi.org/10.1007/s00382-016-3048-0.